LETTERS

Phosphorylation of WAVE1 regulates actin polymerization and dendritic spine morphology

Yong Kim[1], Jee Young Sung[1], Ilaria Ceglia[1], Ko-Woon Lee[1], Jung-Hyuck Ahn[1], Jonathan M. Halford[1], Amie M. Kim[1], Seung P. Kwak[2], Jong Bae Park[3], Sung Ho Ryu[3], Annette Schenck[4], Barbara Bardoni[4], John D. Scott[5], Angus C. Nairn[1,6] & Paul Greengard[1]

WAVE1—the Wiskott–Aldrich syndrome protein (WASP)-family verprolin homologous protein 1—is a key regulator of actin-dependent morphological processes[1] in mammals, through its ability to activate the actin-related protein (Arp2/3) complex. Here we show that WAVE1 is phosphorylated at multiple sites by cyclin-dependent kinase 5 (Cdk5) both *in vitro* and in intact mouse neurons. Phosphorylation of WAVE1 by Cdk5 inhibits its ability to regulate Arp2/3 complex-dependent actin polymerization. Loss of WAVE1 function *in vivo* or in cultured neurons results in a decrease in mature dendritic spines. Expression of a dephosphorylation-mimic mutant of WAVE1 reverses this loss of WAVE1 function in spine morphology, but expression of a phosphorylation-mimic mutant does not. Cyclic AMP (cAMP) signalling reduces phosphorylation of the Cdk5 sites in WAVE1, and increases spine density in a WAVE1-dependent manner. Our data suggest that phosphorylation/dephosphorylation of WAVE1 in neurons has an important role in the formation of the filamentous actin cytoskeleton, and thus in the regulation of dendritic spine morphology.

Cdk5, together with its neuron-specific regulatory subunit P35, has been implicated in neurite outgrowth and neuronal migration during brain development[2,3], in striatal function in mature brain[4], and in Alzheimer's disease[3,5] and drug addiction[6,7]. In view of the growing appreciation of Cdk5 in normal and abnormal neuronal function, we undertook a search for interacting proteins. To identify interacting proteins, purified recombinant P35/Cdk5 protein was immobilized on Protein A beads coupled to anti-P35 antibody, and affinity chromatography was used to isolate proteins from striatal lysates (Fig. 1a). Three major co-precipitated proteins with a relative molecular mass (M_r) of 140,000, 125,000 and 43,000 were identified as PIR121 (p53-inducible messenger RNA), Nap1 (Nck-associated protein 1) and β-actin respectively, by matrix-assisted laser desorption/ionization–time of flight (MALDI-TOF) mass spectrometry (data not shown). Previously, PIR121 and Nap1 were co-purified from bovine brain with WAVE1, Abi2 (Abl interactor 2) and HSPC300 in a pentameric protein complex[8]. The presence of WAVE1 (but not WAVE2 or WAVE3), PIR121 and Nap1 in the complex of P35/Cdk5 binding proteins was confirmed by immunoblotting with specific antibodies (Fig. 1b, Supplementary Fig. 1a). Evidence for the interaction of the WAVE1 complex and P35 was also obtained from co-immunoprecipitation studies: (1) using lysates prepared from cultured neurons (Supplementary Fig. 1b), and (2) after expression of proteins in COS-7 cells (Supplementary Fig. 1c). Direct interaction of P35 (but not Cdk5) with PIR121, Nap1 and WAVE1 was also found using a 'far western' blotting technique (Supplementary Fig. 1d–f), suggesting a critical role for P35 in the interaction with the WAVE1 complex.

Purified WAVE1 complex was incubated without or with purified P35/Cdk5 in the presence of Mg[γ-^{32}P]ATP. In addition to P35 (which is known to be autophosphorylated by Cdk5), WAVE1 was highly phosphorylated, with an upward mobility shift (Fig. 1c). Cdk5 is a so-called proline-directed kinase that phosphorylates serine or threonine residues with an adjacent carboxy-terminal proline residue. Three serines, S310 as the major site (~50% of phosphorylation) and S397 and S441 as minor sites, were identified (Supplementary Fig. 2a). Triple mutations at S310, S397 and S441 abolished ~83% of phosphorylation (data not shown). The three phosphorylation sites are located in the proline-rich region of WAVE1 (Fig. 1d), but are not conserved in WAVE2 or WAVE3 (ref. 9). Phosphorylation by Cdk5 may therefore be specific for WAVE1. However, it is possible that WAVE2 and WAVE3 are phosphorylated at other non-conserved proline-directed sites by Cdk5 or other kinases. We also confirmed the phosphorylation at S310, S397 and S441 using phospho-specific antibodies (Supplementary Fig. 2b, c).

High basal phosphorylation of S310, S397 and S441 was detected in striatal slices (see Supplementary Table 1). Treatment with the Cdk5 inhibitor, roscovitine, resulted in a marked reduction of phosphorylation at each of the three sites (S310, 23%; S397, 11%; S441, 40% of control level with 10 μM roscovitine) (Fig. 1e). Phosphorylation of WAVE1 was not affected by treatment with U0126, an inhibitor of mitogen-activated protein kinase kinase (MAPKK) (Fig. 1e). Phosphorylation of MAPK (another proline-directed kinase) was reduced to near undetectable levels after treatment with U0126, but not with roscovitine. Moreover, analysis of primary cultured cortical neurons from Cdk5-knockout mice revealed a significant reduction of phosphorylation at each of the three sites (S310, 44 ± 11.9%; S397, 18 ± 4.1%; S441, 42 ± 9.7% of wild-type level) (Supplementary Fig. 3). These results indicate that WAVE1 is a physiological substrate for Cdk5, but it also appears that additional kinase(s) phosphorylate WAVE1 in neurons.

WAVE and related WASP proteins have a conserved verprolin-homology, cofilin-homology, acidic (VCA) domain that directly binds to and activates the Arp2/3 complex, resulting in polymerization of actin[10]. The WAVE1 complex purified from rat brain cytosol and recombinant His-WAVE1 were both highly active, and comparable to a GST-VCA domain from WASP in the pyrene actin assay (Supplementary Fig. 4). The high activity of the WAVE1 complex was dependent on WAVE, but not on contaminating WASP proteins. N-WASP was not present in the WAVE1 complexes, as judged by immunoblotting (data not shown). Moreover, pre-incubation of the

[1]Laboratory of Molecular and Cellular Neuroscience, The Rockefeller University, 1230 York Avenue, New York, New York 10021, USA. [2]Discovery Neurosciences, Wyeth Research, Princeton, New Jersey 08543, USA. [3]Division of Molecular and Life Sciences, Pohang University of Science and Technology, Pohang, 790-784, Korea. [4]Institut de Génétique et de Biologie Moléculaire et Cellulaire, CNRS/INSERM/ULP, BP 10142, 67404 Illkirch cedex, France. [5]Howard Hughes Medical Institute, Vollum Institute, 3181 Sam Jackson Park Road, Portland, Oregon 97239-3098, USA. [6]Department of Psychiatry, Yale University School of Medicine, 34 Park Street, New Haven, Connecticut 06508, USA.

WAVE1 complex (or recombinant WAVE1) with an anti-C-terminal WAVE1 antibody abolished Arp2/3-complex-dependent actin polymerization, while having no effect on the activity of the GST-VCA domain from WASP (data not shown). WAVE2 complex reconstituted *in vitro* was also found to be active[11], supporting our conclusion that the WAVE1 complex is active. Our results contrast with a previous result indicating that the WAVE1 complex purified from bovine brain was inactive[8].

We next examined the effect of phosphorylation by Cdk5 on WAVE1-induced Arp2/3-complex-mediated actin polymerization. Pre-incubation of the WAVE1 complex (Fig. 2a) or of recombinant WAVE1 (Fig. 2b) with P35/Cdk5 in the presence of MgATP led to a substantial reduction in actin polymerization compared to that obtained when MgATP was omitted. Notably, basal phosphorylation at S310, S397 and S441 was found in recombinant WAVE1 (insets in Fig. 2b, c, see also Supplementary Table 1). Pre-incubation of recombinant WAVE1 with a non-specific λ protein phosphatase (λPPase) reduced basal phosphorylation and this was accompanied by an increase in WAVE1-mediated actin polymerization (Fig. 2c).

Mutation of S310 (S310A), S397 (S397A), or S441 (S441A) to alanine rendered WAVE1 activity partially resistant to inhibition by Cdk5-dependent phosphorylation: the generation of barbed ends by WAVE1 after phosphorylation was 29%, 72%, 50% and 41% for the wild-type, S310A, S397A, and S441A mutants, respectively, compared to the corresponding unphosphorylated proteins. Combined mutation at S310 and S397 was no more effective than mutation at S310 alone (Fig. 2d and Supplementary Fig. 5b, c). Conversely, λPPase-mediated activation was not observed following mutation of S310A alone or double mutation of S310A and S397A (Fig. 2e and Supplementary Fig. 6). The S310A, S397A, S441A, and S310A:S397A mutants exhibited comparable basal activity to wild-type WAVE1 (Supplementary Fig. 5a). In contrast, a mutant form of WAVE1 where S310 was changed to aspartate (S310D) to mimic phosphorylation exhibited low basal activity that was little affected by incubation with P35/Cdk5 or λPPase (Fig. 2d, e). Altogether, the results indicate that phosphorylation of S310 by Cdk5 is largely responsible for inhibition of WAVE1 activity, with phosphorylation of S397 playing a lesser role and phosphorylation of S441 having little influence.

WASP, as well as the WAVE-binding proteins Abi2 and insulin receptor tyrosine kinase substrate p53 (IRSp53), have been implicated in the regulation of spine morphology[12–14], and formation of branched actin filaments in spine heads[15] probably involves the Arp2/3 complex. However, little is known about the role of WAVE1 in dendritic spine morphology. We next analysed spine morphology of medium spiny neurons in striatal sections obtained from WAVE1$^{-/-}$ mice.

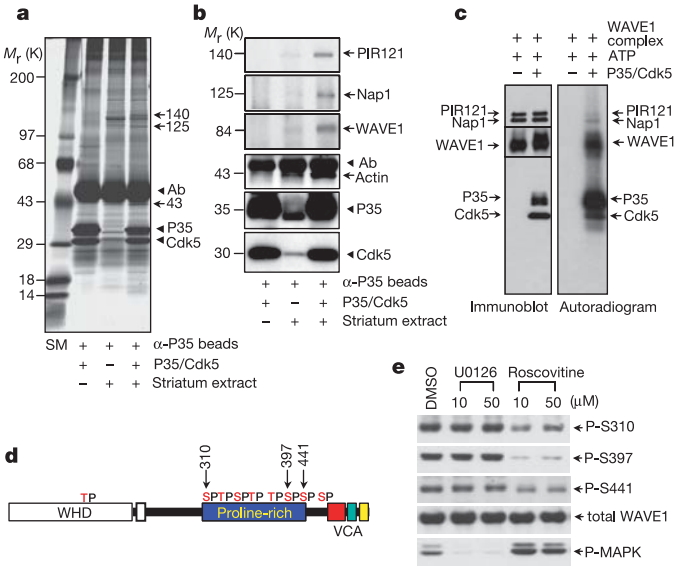

Figure 1 | WAVE1 interacts with, and is phosphorylated by, P35/Cdk5. **a**, **b**, Purified P35/Cdk5 was immobilized on anti-P35 antibody-coupled beads, without or with striatal extract. Bound proteins were visualized with silver stain (**a**) or immunoblotted for the indicated proteins (**b**). Arrowheads indicate immobilized antibody (Ab), P35 or Cdk5. **c**, Purified WAVE1 complex was incubated with [γ-^{32}P]ATP in the absence or presence of P35/Cdk5, and the samples were analysed, following SDS–polyacrylamide gel electrophoresis (SDS–PAGE), by immunoblotting for the indicated proteins, or by autoradiography. **d**, Domain structure of WAVE1 including the proline-rich domain, amino-terminal WAVE homology domain (WHD) and C-terminal VCA domain. Nine TP or SP (threonine-proline or serine-proline) sites are found in both mouse and human WAVE1. Arrows indicate Cdk5 phosphorylation sites. **e**, Striatal slices were incubated for 1 h with DMSO, a Cdk5 inhibitor (roscovitine, 10 μM, 50 μM) or a MAPKK inhibitor (U0126, 10 μM, 50 μM). Phosphorylation of WAVE1 at S310, S397 and S441, total WAVE1, and phospho-MAP kinase (P-MAPK) were analysed by immunoblotting.

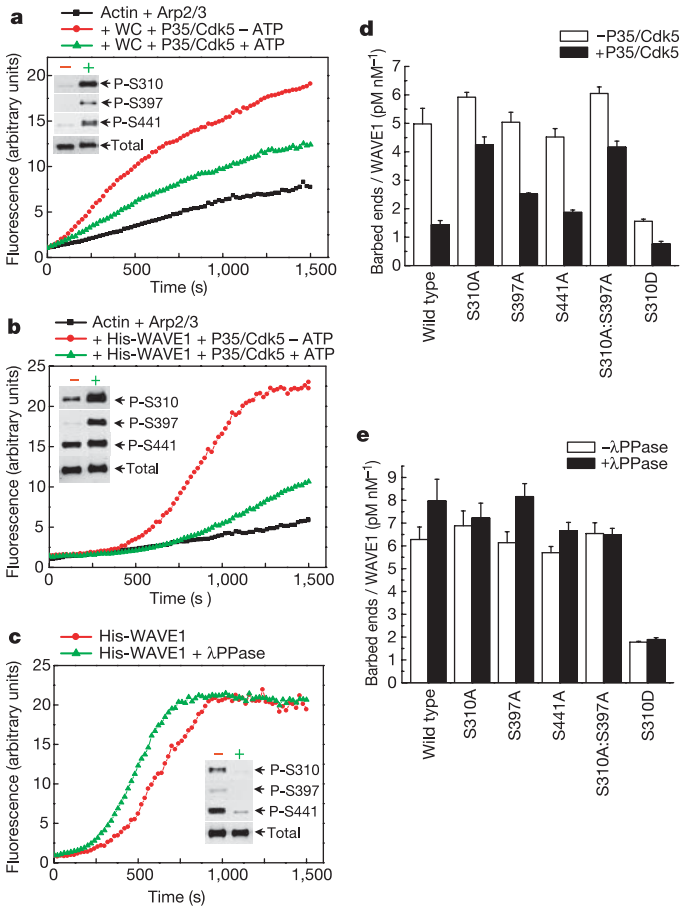

Figure 2 | Inhibition of Arp2/3-complex-mediated actin polymerization by phosphorylation of WAVE1. **a**, **b**, Native WAVE1 complex (WC) (**a**) or recombinant His-WAVE1 (**b**) was pre-incubated with P35/Cdk5 in the absence or presence of MgATP, and a pyrene-actin polymerization assay performed. The lower inhibition of the WAVE1 complex compared to recombinant WAVE1 results from the lower fractional phosphorylation of WAVE1 at S310 in the WAVE1 complex (see Supplementary Table 1). **c**, His-WAVE1 was pre-incubated in the absence or presence of λPPase and actin polymerization was measured. In **a**–**c**, the insets show phospho-WAVE1 and total WAVE1 in the absence (−) and presence (+) of MgATP or λPPase. **d**, **e**, The activity of wild-type WAVE1 or phosphorylation site mutants was measured after (**d**) pre-incubation with MgATP in the absence or presence of P35/Cdk5, or (**e**) with or without λPPase. The barbed-end generation by WAVE1 was calculated from data shown in Supplementary Figs 5b and 6a. Error bars indicate the standard error of the linear regression analysis of data obtained from duplicate actin polymerization assays.

WAVE1$^{-/-}$ neurons displayed a significant reduction in class 1 spines (stubby type), class 2 spines (comprised of mature spines with a relatively large head and a short neck) and class 3 spines (thin spines) and showed a relatively high density of class 4 protrusions, or filopodia (Fig. 3a, b). Similarly, reduced expression of WAVE1 (as a result of RNAi) in primary hippocampal neurons resulted in a decrease in the density of class 2 spines and an increase in filopodia (Fig. 3c, d). Expression of RNAi-resistant wild-type (Rr-WT) WAVE1 (in conjunction with RNAi) reversed the loss of the class 2 spines as well as the increase in filopodia. Notably, expression of a Rr-S310A mutant (to mimic the dephosphorylated active form) had a greater effect than Rr-WT, whereas expression of a Rr-S310D mutant (to mimic the phosphorylated inactive form) had little or no effect on the RNAi-induced phenotype (Fig. 3e, f).

Our results indicate that WAVE1 is phosphorylated at three sites in intact neurons under basal conditions (Supplementary Table 1), reflecting basal activity of Cdk5. Stimulation of striatal slices with the dopamine D1 agonist SKF82526 decreased WAVE1 phosphorylation at S310, S397 and S441 (60 ± 9.1, 29 ± 4.3, 36 ± 11.8% of control, respectively) (Fig. 4a). Similar results were obtained using forskolin to activate the cAMP pathway (Fig. 4b). Activation of the cAMP pathway had no effect on Cdk5 activity (Supplementary Fig. 7), suggesting the involvement of a protein phosphatase in cAMP-mediated WAVE1 dephosphorylation. When pure neuronal cultures of hippocampus were treated with forskolin for 1 h, the level of phosphorylation of all three sites decreased (Fig. 4c). (Similar results were obtained for cortical neurons; data not shown.) This was associated with an increase in the numbers of class 2 and 3 spines as well as class 4 protrusions (Fig. 4d, e). Downregulation of WAVE1 using RNAi abolished the forskolin-induced increase in the number of class 2 and 3 spines (Fig. 4d, e).

The present results indicate that WAVE1 phosphorylation/dephosphorylation plays an important part in the regulation of actin polymerization and dendritic spine morphology. The WAVE proteins

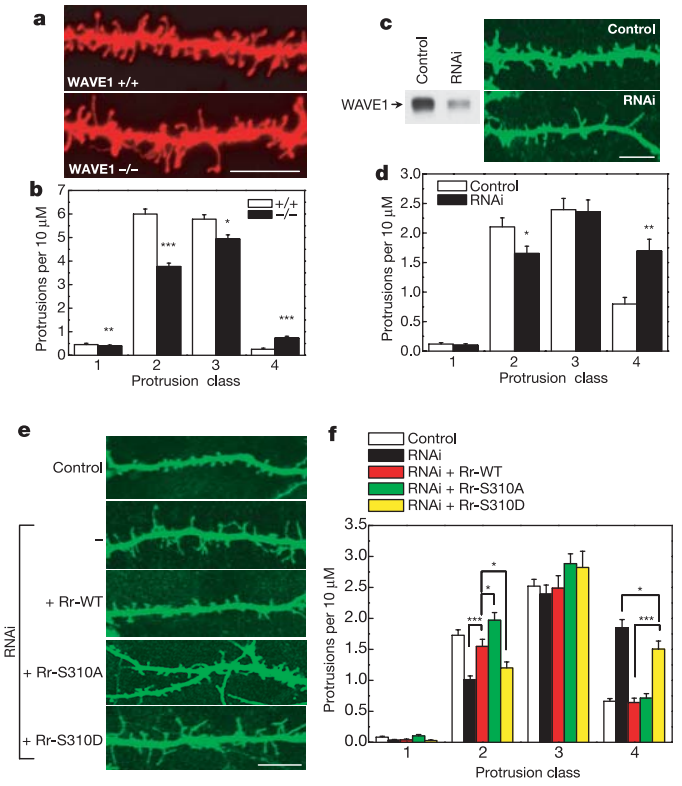

Figure 3 | Role of WAVE1 in spine morphogenesis. **a**, **b**, Spine morphology of medium spiny neurons in striatum of wild-type (+/+) or WAVE1 knockout (−/−) mice (P24) (visualization used DiI staining). **c**, **d**, Primary hippocampal neurons (8 days *in vitro*) were co-transfected with EGFP plus WAVE1-RNAi plasmid (RNAi) or a plasmid vector (Control). Spine morphology (12 days *in vitro*) was visualized in **c** and **e** using anti-GFP antibody. Downregulation of WAVE1 was confirmed by immunoblot analysis of neurons infected with a lentiviral vector containing WAVE1 RNAi (left in **c**). **e**, **f**, Neurons were co-transfected with EGFP plus control plasmid vectors (Control) or plasmids for RNAi and RNAi-resistant WAVE1, as indicated. Wild-type and mutant Rr-WAVE1 transgenes contained an N-terminal Myc-tag and equivalent co-expression of transgenes was observed upon immunostaining of Myc (data not shown). Scale bars in **a**, **c** and **e**, 10 μm. **b**, **d**, **f**, Quantification of protrusion density (number per 10 μm dendrite length; mean ± s.e.m.) in four classes. $^{*}P < 0.05$, $^{**}P < 0.01$, $^{***}P < 0.001$ versus wild type (**b**), Control (**d**), or RNAi or RNAi + Rr-WT as indicated (**f**), Kolmogorov–Smirnov test.

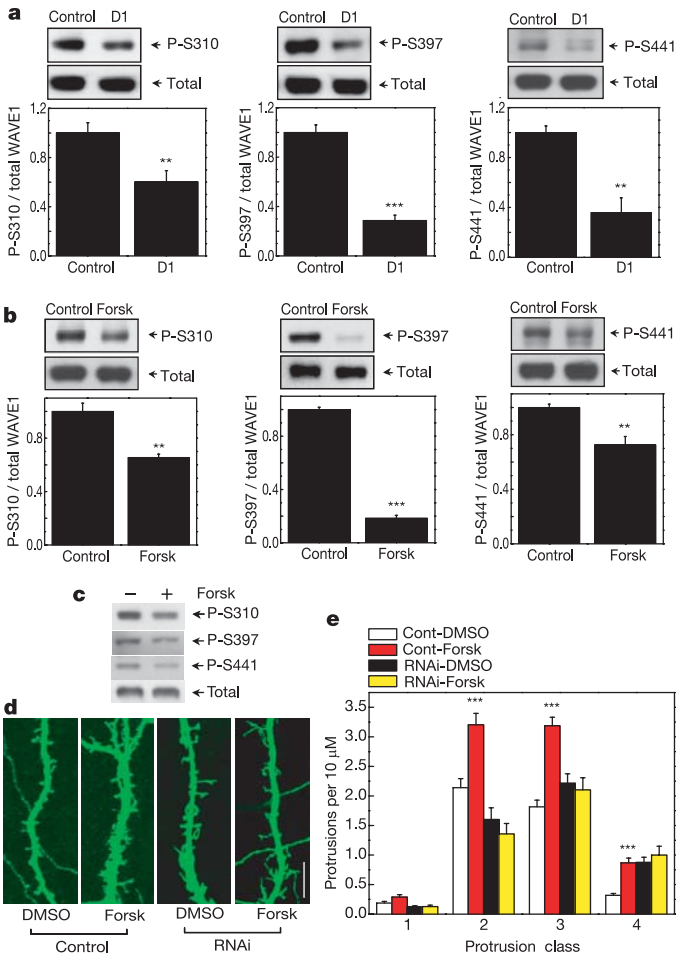

Figure 4 | cAMP-dependent dephosphorylation of WAVE1 and its role in spine formation. **a**, **b**, Striatal slices were incubated in the presence of DMSO (Control), the dopamine D1 receptor agonist SKF82526 (D1, 1 μM) (**a**) or forskolin (Forsk, 1 μM) (**b**) for 30 min. The levels of phospho- and total WAVE1 were measured by immunoblotting (upper panels) and the results quantified by densitometry (lower panels). Data, normalized to control values, represent means ± s.e.m. for four to six experiments. $^{**}P < 0.01$, $^{***}P < 0.001$ versus control, Student's *t* test. **c**, Primary hippocampal neurons were incubated with DMSO (−) or forskolin (+, 1 μM) for 1 h, and phospho-WAVE1 and total WAVE1 visualized by immunoblotting. **d**, **e**, Primary hippocampal neurons were co-transfected with EGFP plus WAVE1-RNAi plasmid (RNAi) or a plasmid vector (Control), and incubated with DMSO or forskolin (Forsk, 1 μM) for 1 h. Dendritic spine morphology was visualized by immunostaining with anti-green fluorescent protein (GFP) antibody. Scale bar, 10 μm. **e**, Quantification of protrusion density (number per 10 μm dendrite length; mean ± s.e.m.) in four classes. $^{***}P < 0.001$ for forskolin versus DMSO, Kolmogorov–Smirnov test.

are activated by Rac[16], a Rho family GTPase, and WAVE1 may be involved in mediating the effects of Rac on spine formation[17,18]. A previous study showed that WAVE1 knockout mice exhibit deficits in learning and memory[19], a phenotype that may be related to the abnormal spine morphology characterized here. Spines contain both bundled and branched forms of filamentous actin[15] and it is likely that WAVE1 contributes to the formation of spines, as well as to remodelling of the actin cytoskeleton in spines during development and in processes affecting synaptic plasticity[20]. In mature neurons in brain or in culture, WAVE1 was highly phosphorylated at Cdk5 sites (S310 and S397 were phosphorylated to stoichiometries of ~0.7 and ~0.9 mol mol^{-1}, respectively, Supplementary Table 1). Stimulation of cAMP-dependent signalling resulted in dephosphorylation of the Cdk5 sites. Thus, WAVE1 would be largely in an inactive form under basal conditions, but would be activated by neurotransmitters, such as dopamine, that increase the levels of cAMP. WAVE1 was found to be required for the effect of cAMP on spine formation, and this probably occurs as a result of cAMP-dependent dephosphorylation and activation of WAVE1. Further clarification of the mechanisms by which Cdk5, cAMP and other signalling pathways regulate WAVE1 phosphorylation/dephosphorylation should lead to an increased understanding of the regulation of spine morphogenesis and synaptic function in developing and adult brain.

METHODS

Pull-down assay. Purified P35/Cdk5 (ref. 21) (20 μg) was incubated with anti-P35 antibody-coupled beads (15 μg antibody/60 μl agarose beads conjugated to protein A). The immobilized P35/Cdk5 was mixed with an extract from ten pooled rat striata homogenized in 20 mM Tris-HCl (pH 7.5), 2 mM $MgCl_2$, 150 mM NaCl, 1% Triton X-100, 30 mM NaF, 1 mM Na_3VO_4, 30 mM $Na_4P_2O_7$ and protease inhibitor cocktail (Roche). After overnight incubation, the beads were precipitated and washed five times with homogenization buffer. Co-precipitated proteins were separated by SDS–PAGE (6–16% acrylamide), followed by silver staining (BioRad) or immunoblotting.

Striatal slices. Striatal slices were prepared from male C57BL/6 mice (6–8 weeks old) as described in ref. 22.

DiI staining. Brain slices from wild-type or $WAVE1^{-/-}$ mice[23] were prepared and labelled with lipophilic fluorescence dye 1,1′-dioctadecyl-3,3,3′,3′-tetramethylindocarbocyanine perchlorate (DiI) as described in ref. 24.

Actin polymerization assay. Pyrene-labelled and non-labelled actin (from rabbit muscle), and Arp2/3 complex were obtained from Cytoskeleton, Inc. WAVE1 complex or recombinant WAVE1 was mixed with Arp2/3 complex (60 nM) in 10 mM Tris (pH 7.5), 50 mM KCl, 1 mM $MgCl_2$, 1 mM EGTA and 0.5 mM ATP. After addition of pyrene-labelled actin (1 μM, 10% labelled), fluorescence was measured at 21 °C in a fluorimeter. The concentration of barbed ends was calculated[25] at the point where polymerization was 50% of the maximum measured within 1,500 s. The concentration of barbed ends measured in the absence of WAVE1 was subtracted from the values calculated in the presence of WAVE1, to obtain measurements of WAVE1-dependent actin polymerization. The concentration of barbed ends generated by wild-type and mutants of WAVE1 was plotted versus WAVE1 concentration, as shown in Supplementary Figs 4d, 5a, 5b and 6a. The data related to the generation of barbed ends by WAVE1 (shown in Fig. 2d and e) was derived from the initial gradient of the slopes shown in Supplementary Figs 5b and 6a.

Image analysis. Acquisition of fluorescence images, morphometric measurements and classification of dendritic spines were as described[24].

Additional information related to DNA constructs, phosphorylation and dephosphorylation of WAVE1 for the actin polymerization assay, cell culture and transfection, and analysis of spines, is included in the Supplementary Methods.

Received 18 April; accepted 6 June 2006.
Published online 16 July 2006.

1. Stradal, T. E. *et al.* Regulation of actin dynamics by WASP and WAVE family proteins. *Trends Cell Biol.* **14,** 303–311 (2004).
2. Smith, D. S., Greer, P. L. & Tsai, L. H. Cdk5 on the brain. *Cell Growth Differ.* **12,** 277–283 (2001).
3. Cruz, J. C. & Tsai, L. H. A Jekyll and Hyde kinase: roles for Cdk5 in brain development and disease. *Curr. Opin. Neurobiol.* **14,** 390–394 (2004).
4. Bibb, J. A. *et al.* Phosphorylation of DARPP-32 by Cdk5 modulates dopamine signalling in neurons. *Nature* **402,** 669–671 (1999).
5. Patrick, G. N. *et al.* Conversion of p35 to p25 deregulates Cdk5 activity and promotes neurodegeneration. *Nature* **402,** 615–622 (1999).
6. Bibb, J. A. *et al.* Effects of chronic exposure to cocaine are regulated by the neuronal protein Cdk5. *Nature* **410,** 376–380 (2001).
7. Norrholm, S. D. *et al.* Cocaine-induced proliferation of dendritic spines in nucleus accumbens is dependent on the activity of cyclin-dependent kinase-5. *Neuroscience* **116,** 19–22 (2003).
8. Eden, S., Rohatgi, R., Podtelejnikov, A. V., Mann, M. & Kirschner, M. W. Mechanism of regulation of WAVE1-induced actin nucleation by Rac1 and Nck. *Nature* **418,** 790–793 (2002).
9. Suetsugu, S., Miki, H. & Takenawa, T. Identification of two human WAVE/SCAR homologues as general actin regulatory molecules which associate with the Arp2/3 complex. *Biochem. Biophys. Res. Commun.* **260,** 296–302 (1999).
10. Takenawa, T. & Miki, H. WASP and WAVE family proteins: key molecules for rapid rearrangement of cortical actin filaments and cell movement. *J. Cell Sci.* **114,** 1801–1809 (2001).
11. Innocenti, M. *et al.* Abi1 is essential for the formation and activation of a WAVE2 signalling complex. *Nature Cell Biol.* **6,** 319–327 (2004).
12. Irie, F. & Yamaguchi, Y. EphB receptors regulate dendritic spine development via intersectin, Cdc42 and N-WASP. *Nature Neurosci.* **5,** 1117–1118 (2002).
13. Grove, M. *et al.* ABI2-deficient mice exhibit defective cell migration, aberrant dendritic spine morphogenesis, and deficits in learning and memory. *Mol. Cell. Biol.* **24,** 10905–10922 (2004).
14. Choi, J. *et al.* Regulation of dendritic spine morphogenesis by insulin receptor substrate 53, a downstream effector of Rac1 and Cdc42 small GTPases. *J. Neurosci.* **25,** 869–879 (2005).
15. Rao, A. & Craig, A. M. Signaling between the actin cytoskeleton and the postsynaptic density of dendritic spines. *Hippocampus* **10,** 527–541 (2000).
16. Miki, H., Suetsugu, S. & Takenawa, T. WAVE, a novel WASP-family protein involved in actin reorganization induced by Rac. *EMBO J.* **17,** 6932–6941 (1998).
17. Luo, L. *et al.* Differential effects of the Rac GTPase on Purkinje cell axons and dendritic trunks and spines. *Nature* **379,** 837–840 (1996).
18. Nakayama, A. Y., Harms, M. B. & Luo, L. Small GTPases Rac and Rho in the maintenance of dendritic spines and branches in hippocampal pyramidal neurons. *J. Neurosci.* **20,** 5329–5338 (2000).
19. Soderling, S. H. *et al.* Loss of WAVE-1 causes sensorimotor retardation and reduced learning and memory in mice. *Proc. Natl Acad. Sci. USA* **100,** 1723–1728 (2003).
20. Matus, A. Actin-based plasticity in dendritic spines. *Science* **290,** 754–758 (2000).
21. Saito, T. *et al.* Developmental regulation of the proteolysis of the p35 cyclin-dependent kinase 5 activator by phosphorylation. *J. Neurosci.* **23,** 1189–1197 (2003).
22. Nishi, A., Snyder, G. L. & Greengard, P. Bidirectional regulation of DARPP-32 phosphorylation by dopamine. *J. Neurosci.* **17,** 8147–8155 (1997).
23. Dahl, J. P. *et al.* Characterization of the WAVE1 knock-out mouse: implications for CNS development. *J. Neurosci.* **23,** 3343–3352 (2003).
24. Lee, K.-W. *et al.* Cocaine-induced dendritic spine formation in D1 and D2 dopamine receptor-containing medium spiny neurons in nucleus accumbens. *Proc. Natl Acad. Sci. USA* **103,** 3399–3404 (2006).
25. Machesky, L. M. *et al.* Scar, a WASp-related protein, activates nucleation of actin filaments by the Arp2/3 complex. *Proc. Natl Acad. Sci. USA* **96,** 3739–3744 (1999).

Supplementary Information is linked to the online version of the paper at www.nature.com/nature.

Acknowledgements We thank W.-B. Gan for assisting us with the DiI staining method; L.-H. Tsai for providing P35 cDNA; A. Yamamoto for Nap1 cDNA; and P. Aspenström for N-WASP antibody. We also thank T. D. Pollard for suggestions. This work was supported by the postdoctoral fellowship programme of the Korea Science & Engineering Foundation (KOSEF) (to J.Y.S.), and funding from the F.M. Kirby foundation (to P.G.), the Picower Foundation (to P.G.), the National Institute of Mental Health, the National Institute of Drug Abuse and the National Institute on Aging (to A.C.N. and P.G.).

Author Contributions Y.K., J.Y.S., I.C. and K.-W.L. performed experiments; J.M.H. and A.M.K. assisted in experiments; J.-H.A., S.P.K., A.S., B.B. and J.D.S. provided reagents; J.B.P. and S.H.R. performed MALDI-TOF mass spectrometry; Y.K., A.C.N. and P.G. designed experiments and wrote the manuscript.

Author Information Reprints and permissions information is available at npg.nature.com/reprintsandpermissions. The authors declare no competing financial interests. Correspondence and requests for materials should be addressed to Y.K. (kimyo@rockefeller.edu), A.C.N. (angus.nairn@yale.edu) and P.G. (greengard@rockefeller.edu).